14-60

INDIAN AND NORTHERN AFFAIRS CANADA
NORTHERN AFFAIRS: YUKON REGION

Open File 1995-14 (G)

GRANITIC PEGMATITES IN THE CANADIAN CORDILLERA: YUKON AND NORTHWEST TERRITORIES

By

LEE A. GROAT
Department of Geological Sciences, University of British Columbia

T. SCOTT ERCIT
Research Division, Canadian Museum of Nature

JAMES K. MORTENSEN and MARK H. F. MAUTHNER
Department of Geological Sciences, University of British Columbia

This report is available from:
Exploration and Geological Services Division,
Indian and Northern Affairs Canada,
300 Main Street, Whitehorse, Yukon Y1A 2B5

GRANITIC PEGMATITES IN THE CANADIAN CORDILLERA: YUKON AND NORTHWEST TERRITORIES

A REPORT SUBMITTED TO THE CANADA/YUKON GEOSCIENCE OFFICE

LEE A. GROAT

Department of Geological Sciences. University of British Columbia

Vancouver, British Columbia V6T 1Z4

T. SCOTT ERCIT

Research Division, Canadian Museum of Nature

Ottawa, Ontario K1P 6P4

JAMES K. MORTENSEN and MARK H.F. MAUTHNER

Department of Geological Sciences. University of British Columbia

Vancouver, British Columbia V6T 1Z4

TABLE OF CONTENTS

1. INTRODUCTION

In this report we describe the results of our research program on granitic pegmatites in Yukon and the western Northwest Territories. These unusual rocks are of scientific and economic interest for the following reasons:

(1) Rare elements such as Ta, Nb, Li, Rb, Cs, Be, and Sn are commonly found in granitic pegmatites, and can occur in concentrations sufficiently high to warrant mining operations (e.g. Bernic Lake, Manitoba). Tantalum and niobium are used in prostheses, capacitors, laser crystals, and piezoelectric instruments; lithium is medicinally important for the treatment of manic depression, is used in advanced technology batteries, and is a key ingredient of specialized glassware (see front-page article in the Globe and Mail, September 26, 1994); and beryllium and tin are industrially important as components of alloys.

(2) Granitic pegmatites host a diversity of rare mineral species, and are a globally important source of gemstones such as emerald, topaz, aquamarine and tourmaline. Pegmatites in western North America have known gemstone potential.

(3) Granitic pegmatites reveal information about melting of rocks in the lower crust and are an important source of information regarding fractionation of felsic magma suites, especially extreme fractionation. The minerals from granitic pegmatites were among the first to be used in absolute (radiometric) dating; granitic pegmatites are of importance in relative and absolute dating of the late stages of tectonic events.

This research project involves the study of granitic pegmatites from the Canadian Cordillera in Yukon and the western part of the Northwest Territories. Considerable research has been done on granitic pegmatite suites from the Canadian Shield; by comparison, the pegmatite potential of the Cordilleran region is largely unknown. This study represents the first attempt ever to conduct original research on the regional geology of Cordilleran pegmatites.

1.1 Granite-Pegmatite Systems

Pegmatites represent end-products of the magmatic stage in the evolution of granitic melts. The appreciable degrees of fractionation required to produce granitic pegmatites can result in significant accumulations of large-ion lithophile elements (LILE) such as lithium, rubidium, and cesium and high field-strength elements (HFSE) such as niobium, tantalum and tin. As such, granitic pegmatites sometimes host economic concentrations of the rare metals lithium, rubidium, cesium, tantalum, niobium, tin and beryllium (e.g., Tanco pegmatite, Manitoba).

Granitoids parental to rare-element-enriched pegmatites ("fertile") have features which distinguish them from other ("barren") granitoids; these features serve both as a prospecting tool for selecting regions worthy of study, and are prophetic of the degree of rare-element enrichment of associated pegmatites. Fertile granites are typically late- to post-tectonic and emplaced at moderate to shallow crustal levels. They are typically texturally inhomogeneous, often with megacrystic ("pegmatoid") pods or regions. They are highly silicic, leucocratic and meta- to peraluminous, often expressed in the accessory mineralogy (cordierite, andalusite or garnet-bearing). They are typically mica-bearing; best prospects are two-mica granites, but biotite granites and, rarely, biotite - hornblende granites have been known to generate rare-element-enriched pegmatites. They generally carry a S-type geochemical signature (White and Chappell, 1983); initial $^{87}Sr/^{86}Sr$ isotopic ratios are high, and K/Rb, K/Cs and K/Li ratios are low.

1.2 Fertile Granites in the Canadian Cordillera

Granitoid rocks are widely distributed in the Canadian Cordillera; however, Sr isotope geochemistry indicates a strong tectonic control over the distribution of evolved granites in the Cordillera. Granitoids with Sr isotopic signatures and trace-element chemistry typical of S-type plutonism (Anderson, 1988) are localized in the Omineca and Foreland Belts. Largely the products of partial melting of older Precambrian and Paleozoic supracrustal rocks during regional compression and thickening, they denote a mid-Cretaceous plutonic event represented in the northern Cordillera by the Selwyn and Cassiar plutonic suites, and in the southern Cordillera by the Bayonne suite. Plutons of the northern suite are occasionally associated with tin-tungsten skarn mineralization. For some of these occurrences, aplite and pegmatite dikes are most abundant in

high-grade ore zones (e.g. Mactung; Atkinson and Baker, 1983); despite extensive work upon skarn mineralization, little has been done to assess the rare element potential of associated pegmatites.

Most of our work to date has been on pegmatites associated with plutons of the Selwyn suite. For this reason, it is appropriate here to consider the general geology of the Selwyn basin.

1.3 General Geology of the Selwyn Basin

The general geology of the Selwyn Basin has most recently been described by Gordey and Anderson (1993), from which the following account of the regional geology is derived. The area that we have been working in (Nahanni map area, 105I) is underlain by late Precambrian to Triassic weakly metamorphised sedimentary rocks. Regional Jurassic-Cretaceous deformation resulted in small- to large-scale, open to tight northwest-trending folds with associated axial-plane cleavage. Plutonic rocks of the region belong to the mid-Cretaceous, calc-alkaline Selwyn suite. The suite consists of radiogenic, metaluminous to peraluminous granitoid rocks. Gordey and Anderson (1993) subdivide the plutonic suite into three groupings: (1) hornblende-bearing plutons, (2) two-mica plutons, and (3) transitional plutons with attributes intermediate to those of (1) and (2). Mineralogical, geochemical, and textural data indicate that the peraluminous, two-mica plutons are the most evolved members of the suite. Contact aureoles about plutonic rocks are typically andalusite- and biotite-bearing; the first appearance of andalusite occurs within one half kilometer of intrusive contacts. Gordey and Anderson (1993) suggest an epizonal to mesozonal depth of emplacement for granitoid plutons in the region. Granitic pegmatites are associated with many of the plutons of the suite, both with hornblende-bearing (metaluminous) and hornblende-free (peraluminous) plutonic rocks.

2. LITERATURE SEARCH

The study began with a comprehensive literature search to identify pegmatites of interest; this involved a computerized GEOSCAN search of assessment reports for Yukon based on the keywords "pegmatite", "spodumene", "beryl", "tourmaline" and "lepidolite". We also used the following characteristics to identify possible fertile granites:

(1) Parent granites are usually isolated, small stocks, typically < 30 km^2 in size; however, they are sometimes found as apophyses and at the margins of larger intrusions (batholiths).

(2) They are S-type granites, meaning that they are derived from supracrustal (often sedimentary) source material (White and Chappell, 1983).

(3) For the Cordillera, fertile granites rich in rare elements are usually mid-Cretaceous in age (Armstrong, 1988).

(4) They are peraluminous (ASI index 1-2), often megacrystic and leucocratic.

(5) They show initial $^{87}Sr/^{86}Sr$ ratios greater than 0.7100 (often 0.7200 to 0.7400) and they have large negative eNd values (typically -6 to -9).

(6) They often have a peraluminous accessory mineralogy (two-mica granites, garnet- or andalusite- bearing) or rare-element bearing accessory mineralization (lepidolite = lithium).

(7) Their whole-rock geochemistry is rich in LILE and HFSE.

Using these criteria, we identified a number of areas of interest. These include the Little Nahanni pegmatite group (which we had worked on in 1992 and 1993), the McQuesten River area, the O'Grady batholith, the Clea pluton, and the Ice Lakes area. All of these areas were investigated in 1994. Areas of interest that we did not have time to study include the Seagull batholith, Thirtymile pluton and Ork stock, Mount Mye batholith, Lened, CAC, and RUDI plutons, the Sekwi Mountain map area, Macmillan Pass, the Whitehorse map area, and Emerald Lake (Fig. 1).

3. PREVIOUS WORK AND THE 1994 FIELD SEASON

The study began in early 1992. That summer we spent a week at Cassiar Beryl in the Horseranch Range, northern British Columbia, and a week at what is now known as the Little Nahanni Pegmatite Group. In 1993 we returned to the LNPG area for a month. In 1994 we spent a final

week in the LNPG area and a week each at the O'Grady batholith, the Clea pluton, and the Ice Lakes area. Two of us (LAG and TSE) also spent several days in the McQuesten River area.

4. ANALYTICAL METHODS

Electron microprobe analyses were done at the Canadian Museum of Nature, and involved a JEOL 733 microprobe with Tracor-Northern 5500 and 5600 automation. Operating conditions were 15 kV and 20 nA, maximum count time 25 s. Data were reduced with a conventional ZAF routine. Undetected constituents (Li_2O, B_2O_3, BeO and H_2O) were calculated according to mineral stoichiometry. The results are given in Appendix 1.

5. LITTLE NAHANNI PEGMATITE GROUP (NWT; 62°12' N, 128°50'W)

5.1 Geological Setting

The granitic pegmatites are located in an unnamed mountain range bound to the northeast by the March Fault and to the southwest by Steel Creek. The dominant structural features of the range are the Fork Anticline and the Summit Syncline, major features of the Selwyn Fold Belt (Gordey and Anderson, 1993). The folds trend northwest-southeast, and plunge to the northwest. The pegmatites are localized in the northeast arm to axial sections of the Fork Anticline. In general, they strike northwest; *i.e.*, subparallel to the strike of axial planes of the fold system. They are dominantly hosted by calcareous metasedimentary rocks of the upper Yusezyu Formation, which consist of mildly metamorphosed equivalents of limestone, variably calcareous sandstone and shale. Granitic plutons are unexposed in the vicinity of the pegmatite group. Syntectonic metamorphism in the immediate study area, however, occurred at an anomalously high grade for this region. Andalusite porphyroblasts occur scattered throughout the metasedimentary rocks, and appear to be coarser in areas to the north of the pegmatite group. Late-tectonic porphyroblasts of staurolite and corderite, and chlorite pseudomorphs after garnet (?), indicate that the area experienced syntectonic metamorphism at temperatures in excess of 500°C. This may reflect the existence of a pluton at shallow levels below the present erosional surface.

5.2 Description of the Pegmatites

5.2.1 Field Relations

The pegmatites range from tabular to lenticular in shape. They have high aspect ratios; individual dikes are a maximum of a few meters in width yet can extend for several kilometers along strike. Contacts are typically sharp, sometimes irregular depending upon the type of host rock. Pegmatites emplaced in calcareous metasedimentary rocks show low degrees of assimilation as evidenced by calcite-lined fractures and late calcium-rich mineral assemblages (often including apatite). Pegmatites emplaced in pelitic metasedimentary rocks often have wide (up to 10 cm) exomorphic aureoles rich in coarse silvery mica or narrow (several mm) bands of black tourmaline. The pegmatites show no mineralogically obvious signs of regional zoning over the 10 km extent of the group.

The pegmatites appear to be synchronous to late in the timing of the last tectonic event to affect the region: dike attitude and shape is variable, ranging from moderately-dipping, contorted and conformable to sedimentary layering to sub-vertical, tabular, undeformed and cross-cutting host strata. The pegmatite group is lithium-rich; the mineralogy and style of internal zoning indicates the group to belong to the albite-spodumene type of the rare-element class of granitic pegmatites (Cerny, 1991).

5.2.2 Mineralogy and Internal Zoning

The dominant minerals of the pegmatite dikes are quartz, potassium feldspar, and albite. Subordinate to these are spodumene, then lepidolite, the dominant carriers of lithium. The spodumene seems to contain trace quantities of manganese, as evidenced by the pink colour of weathered samples, and by the concentration of black manganese oxides along fracture planes. Spodumene and K-feldspar are typically the coarsest phases, with individual crystals often greater than 10 cm in length, and account for the pegmatitic texture of most dikes. Albite is variable in size and texture; mostly it is saccharoidal in texture, but in places is coarsely cleavelanditic. Lepidolite is similarly variable, comparable in size to saccharoidal albite in aplitic sections of dikes, but ranging to coarse-grained "ball-peen" (colliform) lepidolite in pegmatitic sections of

some dikes. Accessory minerals include tantalian rutile and cassiterite, columbite-group minerals, Mn-bearing apatite, lithiophilite, amblygonite-montebrasite, and beryl. Preliminary electron microprobe work shows that many of the oxide phases are strongly oscillatorily zoned.

Internal zoning of the pegmatites ranges from simple to chaotic. Where simple, the outward to inward succession of zones consists of a narrow border unit, one to two wall units, an irregularly-zoned intermediate unit, and uncommonly, a quartz core. Where chaotic, there is less of a distinction between wall and intermediate units as expressed by alternations of aplitic and pegmatitic layers. At contacts there is a thin fine-grained border unit rich in plagioclase and muscovite. The wall unit dominantly consists of plagioclase and quartz, with lesser amounts of K-feldspar. Pegmatites emplaced in pelitic metasediments have two wall units, the outermost of which has relatively higher concentrations of muscovite or lepidolite. Wall units vary considerably in thickness and texture but are typically several cm in width and aplitic in texture. The contact between the wall unit and the intermediate unit is not sharp, but is defined by a coarsening of mineral textures towards the centres of dikes. For many dikes, the first appearance of spodumene can be used as a reliable indicator of the start of the intermediate unit. In general, the intermediate unit consists of K-feldspar, plagioclase, quartz, spodumene, with or without lepidolite. The appearance or absence of lepidolite can simply be explained as being due to slight variations in m HF, pushing phase relations in and out of the lepidolite-stable field (London, 1984). The intermediate unit is typically rhythmically banded; this banding is expressed in two ways: (1) as alternations of pegmatitic and aplitic layers, and (2) as variations in modal mineralogy of aplitic layers. Aplitic layers are similar in mineralogy and texture to the wall unit. Pegmatitic layers consist of coarse-grained K-feldspar, spodumene, and quartz with or without lepidolite. Directional crystal growth is strongly expressed by (1) banding in the aplitic layers, which is parallel to dike contacts, and by (2) elongate K-feldspar and spodumene crystals in the pegmatitic layers, which are perpendicular to dike contacts. Monomineralic quartz cores are rare and occupy central portions of the dikes.

5.2.3 Geochemistry and Petrogenesis

The pegmatite dikes are peraluminous. The dikes show an overall predominance of lithophile elements; they are strongly enriched in lithium and fluorine, weakly enriched in phosphorus,

manganese, beryllium, tantalum, and niobium. The absence of tourmaline (except at exocontacts) indicates that the pegmatites are poor in boron. Preliminary microprobe analyses of oxide phases show that the dikes are enriched in Mn with respect to Fe, and in Ta with respect to Nb. Thus, in terms of mineralogy and preliminary geochemistry, the group is part of the LCT (*Li-Cs-Ta*) geochemical suite of granitic pegmatites (Cerny, 1991). The sporadic occurrence of goshenite beryl implies a possible Cs enrichment, to be tested in later geochemical studies.

Phase relations amongst the lithium aluminosilicates can be used to apply preliminary petrogenetic constraints to pegmatite evolution (London, 1984). The absence of (1) primary petalite, (2) secondary spodumene plus quartz intergrowths, and (3) eucryptite, in the presence of primary spodumene plus quartz, implies relatively low T/moderate P emplacement conditions for the pegmatitic melts *(circa* 3 to 3.5 kb, 550-650°C).

5.3 Geochronology

5.3.1 Introduction

Most of the pegmatites contain muscovite and/or lepidolite, which was separated for K-Ar dating. No zircon, titanite or monazite have been found in the pegmatites; hence we considered analyzing other accessory phases such as columbite or cassiterite. Many of the cassiterite grains examined during electron microprobe studies contain abundant inclusions, rendering them unsuitable for dating purposes. Columbite, however, was relatively inclusion-free, with the exception of rare inclusions of wodginite-group minerals, tantalian rutile and an unknown uranium oxide which were identified in microprobe studies of a few columbite samples. U-Pb dating studies using columbite have previously been described by Aldrich *et al.* (1956) and Romer and Wright (1992), who determined U-Pb ages for columbites from two pegmatite bodies and a metamorphic aureole in Sweden. The columbite ages obtained in previous studies were in good agreement with U-Pb zircon and titanite ages from related rock units. Romer and Wright (1992) inferred a relatively high closure temperature (greater than lower amphibolite grade) for the U-Pb system in columbite. As columbite has only been used twice before for U-Pb dating and never on rocks as young as those examined in this study, K-Ar ages were obtained from lepidolite and muscovite in an attempt

to corroborate the ages obtained from the columbites. Analytical methods and sample descriptions are given in Mauthner *et al.* (1995).

5.3.2 Results

U-Pb analyses of nine fractions of columbite were completed, comprising three fractions from each of three samples. The Pb isotopic composition of coexisting albite was also measured for each of the three samples, and used as an estimate for the initial common Pb composition for data reductions. Measured U-contents for the columbites range from 279 to 1383 ppm, with all but one of the fractions containing between 279 and 947 ppm U. The fraction with an anomalously high U-content is thought to have contained microscopic inclusions of the unknown U-oxide mineral. Most of the fractions contain a significant proportion of common Pb (2.5 to 5.5%). Th/U ratios for each analysis, calculated using measured $^{208}Pb/^{204}Pb$ and $^{206}Pb/^{204}Pb$ ratios and an assumed age of 82 Ma, are very low (≤ 0.01). This is considerably lower than the Th/U ratios reported by Romer and Wright (1992) for columbites analyzed in their study. The nine analyses are plotted on a conventional concordia plot in Figure 2. Seven of the fractions plot on or near concordia at about 82 Ma. Two of the fractions (233-A and 233-C) give slightly lower $^{206}Pb/^{238}U$ ages. The data are replotted on $^{238}U/^{204}Pb$ vs. $^{206}Pb/^{204}Pb$ isochron diagrams in Figures 3(a) to (d). Isochron ages calculated for each of the samples, using the measured Pb isotopic composition of coexisting feldspar to fix the initial $^{206}Pb/^{204}Pb$ ratio, are as follows: sample 113, 82.2 ± 0.3 Ma (MSWD = 0.2); sample 167, 81.6 ± 0.5 Ma (MSWD = 7.6); and sample 233, 81.6 ± 2.3 Ma (MSWD = 19.3). An age calculated using all seven columbite analyses alone is 81.6 ± 0.5 (MSWD = 7.9) with a calculated initial ratio of 20.22. The Pb isotopic compositions of the feldspars are highly radiogenic; they plot somewhat above the "shale curve" of Godwin and Sinclair (1982), which is an average crustal growth curve for mid-Proterozoic and younger sedimentary units in the miogeocline in northwestern North America. This suggests that the pegmatites represent crustal melts, which is in keeping with their peraluminous or "S-type" character inferred from their mineralogy.

With respect to the K-Ar study the muscovite sample (sample 235) gave an age of 65.4 ± 4.0 Ma and the two lepidolite samples (samples 197 and 230) gave ages of 65.8 ± 3.4 Ma and 65.4 ± 3.6 Ma.

Both the U-Pb and K-Ar ages obtained in this study are surprisingly young. We interpret the K-Ar mica ages as the time at which the pegmatite bodies last passed through the blocking temperature of the K-Ar system in muscovite and lepidolite (~350°C). There are three possible ways to interpret the U-Pb columbite ages; either (1) as emplacement ages of the pegmatites; (2) as cooling ages at some time following emplacement; or (3) as thermally reset ages. The timing of pegmatite emplacement is interpreted to be late syntectonic, and the pegmatites intrude wall rocks that have experienced metamorphic temperatures in excess of 500°C. We consider it highly unlikely, however, that pegmatite samples from three widely separated (up to 3.5 km apart) localities would yield identical regional, post-metamorphic cooling ages. The relatively high closure temperature inferred for the U-Pb system in columbite by Romer and Wright (1992) also argues against the U-Pb values being cooling ages. Similarly the identical U-Pb columbite ages are unlikely to represent resetting related to the same thermal event that reset the K-Ar mica ages. The U-Pb ages must therefore either represent either an older, high-temperature thermal event that completely reset the U-Pb columbite systems or the actual emplacement ages of the pegmatite bodies. The U-Pb columbite ages are 8 to 13 m.y. younger than any isotopic ages obtained thus far for other granitic intrusions in this region; however the pegmatites are also mineralogically distinct from any of the other plutonic rocks. In the absence of any evidence for a ~82 Ma thermal event in this region, we therefore interpret the U-Pb columbite ages to date the emplacement of the pegmatites. This indicates that the pegmatites represent a magmatic event that has not previously been recognized. The Pb isotopic compositions of feldspars in the pegmatites suggest that the magmas are entirely crustally-derived, and it is therefore likely that the magmas represent small volumes of initial partial melt material formed during regional metamorphism. A metamorphic event of this age has also not been recognized in this area, although the Mackenzie fold-and-thrust belt was presumably still active at this time (Gordey and Anderson, 1993).

The Late Cretaceous-Paleocene K-Ar mica ages for the pegmatites probably reflects a thermal overprint related to a relatively young intrusive event. No plutons of this age have been recognized thus far in the immediate study area; however K-Ar biotite ages in the range of 60 to 69 Ma were obtained for two small granitoids about 100 km southeast of the study area (D.A. Archibald, unpublished data). These ages are consistent with U-Pb zircon and monazite and K-Ar biotite ages obtained from plutons of the McQuesten plutonic suite in the McQuesten River area in west-central Yukon (Murphy and Héon, 1994; Murphy *et al.*, in press). It is of interest to note that plutons of

the McQuesten suite and the area of known Late Cretaceous-Paleocene intrusions and thermal overprinting in and near our study area occupy roughly equivalent positions within the overall arc of the Mackenzie fold-and-thrust belt.

6. OTHER AREAS

6.1 McQuesten River Region, Central Yukon (63°47'N, 137°25'W)

Two-mica granites in the McQuesten River region of central Yukon are similar to those in the Selwyn Suite, thus are potentially parental to rare-element pegmatites (JKM, work in progress). LAG and TSE spent several days in late July, 1994, studying granitoid plutons in the area, in the company of D. Murphy and JKM. Subsequent to this, we examined an additional pluton in the area (the Two Sisters batholith) in detail. The Two Sisters batholith is a late Cretaceous (65 Ma), medium to coarse grained, locally porphyritic two-mica granite. We examined the northern margin of the batholith, where a megacrystic marginal phase is exposed. Numerous small, black tourmaline-bearing, coarse-grained segregations are present in the marginal phase, but pegmatites *sensu stricto* are conspicuously absent. The presence of tourmaline in the segregations indicates local enrichment in boron, which is a potential indicator of rare-metal enrichment. However, there are no mineralogical indicators of rare-metal mineralization (*i.e.*, no rare-metal oxides of Sn, Ta or Nb, nor coloured tourmaline indicative of Li enrichment). Whole rock and mineral analyses (currently underway) are anticipated to confirm these observations.

6.2 O'Grady Batholith (NWT; 62°45'-53'N, 128°30'-129°15'W)

The O'Grady batholith (270 km^2) is made up of three phases; a predominant, megacrystic quartz syenite core, and subordinate transitional and marginal hornblende biotite granodiorite and quartz syenite phases arranged concentrically around the core. Tourmaline-bearing, rarely miarolitic, aplite and granitic pegmatite dikes are widespread, especially in the core phase (Gordey and Anderson, 1993).

We spent one week on the western margin of the O'Grady batholith in August, 1994. Pegmatite and aplite dikes are abundant along this margin, and are concentrated in a 12 km long by 1 km

wide band in the quartz syenite core (Fig. 4). Mapping and sampling activities covered 80% of the pegmatite-rich band. The quartz syenite host is remarkably homogeneous over the investigated region; the only obvious field variation is in the modal abundance of hornblende.

Aplite dikes show uniform characteristics: fine-grained, plagioclase-feldspar-rich, moderately boron-rich (abundant tourmaline). The dikes are typically small (1 metre to, exceptionally, a few m in width), and often occur in en-echelon swarms.

The vast majority of granitic pegmatites have the following characteristics: (1) Coarse-grained (crystal size often exceeds 10 cm); (2) Boron-rich, as typified by abundant tourmaline and sporadic axinite; (3) Often LREE-enriched, as typified by uncommon allanite; (4) Simple internal zonation; the typical margin-to-core sequence is: border unit (feldspar-rich), wall unit (graphic K-feldspar + quartz ± plagioclase feldspar), intermediate unit (blocky K-feldspar, quartz) and quartz core (commonly miarolitic). Pegmatites at topographically high levels of the batholith are locally enriched in lithium, as evidenced by the occurrence of lepidolite and gem-quality coloured tourmaline. The gem tourmaline is of cutting grade; we strongly advise commercial development of the lithium pegmatites of the batholith. Based on published geochemical models for fertile granites and their pegmatites, lithium enrichment was a completely unanticipated geochemical trend for the batholith. We are investigating two models for lithium enrichment; extreme fractionation *versus* assimilation. Detailed geochemical and geochronological investigations on the O'Grady batholith and its pegmatites are currently in progress.

Satellitic dikes on the western margin of the batholith were investigated. We had anticipated that such dikes would represent exterior pegmatites (*i.e.*, exterior to the O'Grady batholith), which, according to current prospecting models for pegmatite deposits, should be more rare-metal-enriched than the interior to marginal pegmatites. All investigated satellitic dikes are aphanitic in texture (*i.e.*, non-pegmatitic). By inference, either exterior pegmatite dikes are absent (*i.e.*, perhaps the finer-grained marginal phases of the batholith were impermeable to pegmatitic melts, thus trapping the pegmatites within the confines of the current-day batholith), or all significant migration of pegmatite melts was upward, and erosion has removed all traces of resultant dikes. Geochemical investigations of the satellitic dikes are to start later this year.

6.2.1 Mineral Chemistry

Tourmaline. Most analytical work focused on variations in tourmaline chemistry, as tourmaline is the main indicator mineral of Li enrichment in the dikes. Selected aspects of tourmaline geochemistry are shown as a function of the fractionation indicator Mn/(Mn+Fe) in Figure 5. Samples with Mn/(Mn+Fe) less than 0.05 represent dikes which host only schorl; samples with Mn/(Mn+Fe) greater than this value represent Li-rich dikes which host coloured tourmaline ± lepidolite. Consistent behaviour is shown by tourmaline samples from the various dikes: Mn, F, and Li behave incompatibly, and Fe, Ti, and Mg behave strongly compatibly. These are normal fractionation trends for LCT-class granitic pegmatites. Combined field and laboratory investigations indicate that the following tourmaline characteristics can be used as inexpensive assessments of Li-enrichment for dikes in the area: (1) the presence of pale-coloured tourmaline (green, pink, colourless), and (2) compositions depleted in Ti, Fe, and Mg. The high degree of correlation of F/(F+OH) with incompatible cation concentrations may indicate that incompatible metal activities are regulated by fluorine contents of the melts (*cf.* Keppler, 1993).

Feldspar. Plagioclase in these dikes is extremely sodic, with compositions ranging from An_0 to An_4. K-feldspar (microcline) is only weakly to moderately enriched in large-ion lithophile elements. The analyses seem to indicate that samples from Li-enriched dikes are more enriched in LILE (Rb, Cs) than samples from Li-poor dikes; *i.e.* the former dikes represent higher degrees of fractionation. K/Rb ratios for K-feldspar are not exceptional. They range from 245 (Li-poor dike) to 60 (Li-enriched dikes), a bit outside the range shown by the batholith (150 ± 25, Gordey and Anderson, 1993), and typical of moderately-lithophile-fractionated pegmatite dikes (Cerny *et al.*, 1985).

Lepidolite. Lepidolite is the second-most abundant carrier of Li in these dikes, and is recognized by its characteristic violet colour. As a species, lepidolite can show a broad range of Al:Li ratios. The analyzed sample (Appendix 1) shows high degrees of Li enrichment, and is moderately enriched in Cs (K/Cs = 26), reflective of its late timing in the crystallization history of the Li-enriched pegmatite dikes (always as a pocket phase).

Titanite. Titanite samples show low to moderate degrees of enrichment in Ta and Nb (to 2.3 wt.% $Nb_2O_5 + Ta_2O_5$) and moderate to high degrees of enrichment in F (to 1.25 wt.% F). These points are consistent with other data for the dikes, indicating the pegmatite melts to be F-rich, yet conspicuously poor in HFSE such as Ta, Nb, Sn or W.

Zircon. Only one zircon crystal was analyzed. The results are shown in Figure 6, a plot of zircon geochemistry as a function of U/(U+Th) and mineral zonation. The zircon sample is enriched in U, Th, Y+HREE, and moderately to weakly enriched in Hf. Core to rim zonation shows that (1) crystal-melt systematics were not sufficient to result in significant Zr-Hf fractionation, (2) total actinide element content diminishes with increasing U-Th fractionation, and (3) Y+HREE behave compatibly.

Hambergite. Hambergite is the sole concentrator of beryllium in the dikes. It is rare, found only in the most fractionated Li-enriched dikes. Only moderate enrichment in F *vs*. OH is shown by the analyzed sample.

Axinite. Axinite is low in abundance in all dikes, but occurs in many dikes in the area. Axinite is recognized by its euhedral, bladed crystals, and pale violet-grey colour. The presence of axinite in conjunction with tourmaline indicates that the dikes show high degrees of boron enrichment. The analyzed sample comes from a schorl-bearing dike and, like schorl, shows high degrees of iron enrichment.

6.2.2 Discussion

From a geochemical viewpoint, the association of lithium-enriched pegmatite dikes with the O'Grady batholith is highly unusual. Previous work has indicated the batholith to show only low degrees of fractionation: it is at most metaluminous, the most fractionated unit of the batholith is a hornblende-bearing quartz syenite, and trace-element chemistry is unexceptional (Gordey and Anderson 1993). The question exists as to how lithium enrichment came about: by extreme fractionation of a rather unexceptional parent, or by assimilation of lithium- and boron-enriched overlying metasediments. The coincidence of lithium and boron enrichment, the localized occurrence of lithium-enriched dikes, and the geochemical unsuitability of the quartz-syenite host

to the dikes as an immediate parent to lithium and boron-enriched pegmatite dikes could be cited as supporting an assimilation origin. However, detailed mineral geochemistry indicates that strong fractionation is at work here. In addition to lithium and boron enrichment, the Li-enriched dikes show (1) strong depletion in Fe, Mg, Ti, REE, (2) moderate enrichment in Mn, F and - as shown by the presence of hambergite - in Be, and (3) relative enrichment in LILE. Together these indicate that high degrees of fractionation are responsible for the Li-enriched dikes. It is still difficult to conceive of a magma now represented by the quartz syenite as directly generating dikes of these compositions by fractionation. Instead, a more evolved (direct) parent is called for. Further, as field relations imply that current erosional levels for the batholith are near the upper margin, the chances seem good for other (*i.e.*, more evolved) phases of the batholith below the current erosional surface.

6.3 Clea Pluton, Selwyn Plutonic Suite, Yukon (62°46.5'N, 129°52'W)

The Clea pluton is a small (0.3 km^2 in exposure), massive to weakly foliated two-mica granite, and is another member of the Selwyn plutonic suite. It is associated with a tungsten skarn (described by Tompson, 1978, and Godwin *et al.*, 1980). Anderson (1983) divides this pluton into equigranular and coarsely megacrystic phases. Pegmatite seams and pods intrude both phases and the scheelite-bearing skarns.

We spent one week at the Clea pluton in August, 1994. Three types of marginal to satellitic dikes were observed and sampled: aphanite (alaskite), aplite, and granitic pegmatite dikes. Aphanite and aplite dikes are intersected by hydrothermal quartz veins which host low concentrations of tungsten mineralization. We found pegmatite dikes to be extremely uncommon and small (to 1 m thick). The few dikes exposed in outcop have irregular contacts, are pod-like in shape, simple in geochemistry and mineralogy (no concentrations of rare metals), and are simply zoned (concentric border, wall, intermediate, and quartz zones). Biotite is the only mica associated with the pegmatite dikes. None of the exposed pegmatite dikes host any W-mineralization or show cross-cutting relationships with hydrothermal veins.

We had hoped that pegmatite would be reasonably abundant or geochemically complex to (1) test models on the timing of pegmatite generation and generation of hydrothermal W mineralization,

and (2) assess the economic potential of pegmatite deposits associated with W-mineralized granites of the Yukon. Clea does not provide these answers, and casts an unfavourable light on the economic potential of pegmatites associated with W-mineralized granites and their deposits. It does, however, raise many questions about the timing and role of water saturation in granitic melts parental to rare-metal (Sn, W) hydrothermal deposits.

6.3.1 Mineral Chemistry

As all granitic pegmatites hosted by the Clea pluton were barren and devoid of exotic accessory phases, all analytical work concentrated on previously unstudied accessory phases in a number of hydrothermal deposits in and about the pluton. The results are given in Appendix 1. Mineral chemistry is, on the whole, unexceptional. Cassiterite is mildly tantalian and titanian, well below extremes shown by granites and associated deposits. Tungsten oxide minerals (scheelite and wolframite) are impoverished in trace HFSE such as Ta and Nb, and show low to moderate Fe/Mn ratios (2.7 in wolframite). All apatite samples are fluorapatite; Cl is conspicuously absent in these samples, and transition metal contents (*e.g.*, Mn, Fe) of the samples are low. Given the barren pegmatite dikes, the lack of any direct association of pegmatite dikes with hydrothermal deposits, the lack of a common HFSE-bearing accessory mineralogy of pegmatite dikes and hydrothermal deposits, and the unexceptional chemistry of accessory oxides and phosphate minerals in the hydrothermal deposits, little can be said about the relative timing and relationship of pegmatite-generating events and the main hydrothermal event at Clea.

6.4 Ice Lakes Area, Cassiar Batholith, Yukon (60°22.5'N, 131°20'W)

The Cassiar batholith is known for associated tin skarns, but very little is known of the beryllium potential of the batholith. Mulligan (1968) was the first to note the association of beryllium mineralization with the Cassiar batholith, in the form of an occurrence of beryl within a single pegmatite dike. Consequently, previous to our studies, nothing was known of the extent or relative concentration of beryllium in the batholith.

We spent one week at the locality in August, 1994. Field activities centred on Mulligan's occurrence, south of the Ice Lakes. A region 6 km by 3 km was investigated, sampled and mapped, and the occurrence of beryllium-bearing pegmatites was delimited (Fig. 7).

Granitic pegmatites are common in the area; aplite dikes are distinctly less common than the pegmatites. All pegmatites are hosted by the batholith; field relations suggest that the area of investigation represents an upper margin of the batholith. The host granite is variable in texture, ranging from fine-grained to megacrystic and sometimes pegmatoid, and unsheared to distinctly sheared; it shows many of the field characteristics expected of granites parental to pegmatite fields. Pegmatite distribution is zoned; NNE to SSW traverses show the following zonation sequence: pegmatite-free $\Rightarrow$ barren-pegmatite $\Rightarrow$ biotite + muscovite-bearing pegmatite $\Rightarrow$ beryl-bearing pegmatite $\Rightarrow$ biotite + muscovite-bearing pegmatite. Exposures to the extreme SSW are too poor to trace pegmatite zonation past the last sequence in the zonation scheme. In general, beryllium-enriched pegmatites are localized in a NNW to SSE trending topographic high in this part of the batholith.

Pegmatites are most commonly as dikes, less commonly as irregular pods. They are typically inextensive along strike (<10 m) and less than 0.5 m thick. The pegmatites tend to be well zoned; the usual margin to core sequence is (1) narrow plagioclase-rich border zone, (2) graphic K-feldspar + quartz $\pm$ 2 mica plagioclase wall zone, (3) blocky K-feldspar + quartz intermediate zone, and (4) a quartz core. Plumose muscovite is sometimes found at the wall zone-intermediate zone contact. Accessory phases include beryl, allanite and magnetite. Cross-cutting relationships indicate the aplite to be younger than the pegmatites.

Beryl crystals range to 5 cm in length, and beryl-bearing pegmatites are common in the area; however, the concentration of beryl in these pegmatite bodies is generally low. Because of the anticipated low grades of beryllium, the deposit is unlikely to be of economic value. Furthermore, while the large tonnage, low-cost Spor Mountain deposit in Utah is in production, (annually supplying approximately 60% of the world's beryllium), North American pegmatitic deposits of beryllium will remain subeconomic. Having said this, we do, however, consider the occurrence of beryllium-bearing pegmatites in the interior of the intrusion a positive economic sign, and advise

further exploration work on known marginal to exterior pegmatites at the eastern contact of the batholith (GSC Map 22-1957).

7. SCIENTIFIC COMMUNICATIONS

7.1 Publications Submitted to Refereed Journals

Mauthner, M.H.F., Mortensen, J.K., Groat, L.A., and Ercit, T.S. (1995): Geochronology of the Little Nahanni Pegmatite Group, Selwyn Mountains, Southwestern Northwest Territories. Submitted to the *Canadian Journal of Earth Sciences* (February 1, 1995).

A paper on the oxide mineralogy of the LNPG is in preparation; this will be submitted to *Geochimica et Cosmochimica Acta* in July.

7.2 Non-Refereed Publications

Groat, L.A., Ercit, T.S., Raudsepp, M., and Mauthner, M.H.F. (1994): Geology and Mineralogy of the Little Nahanni Pegmatite Group. Department of Indian Affairs and Northern Development Report 1994-14.

7.3 Refereed Conference Abstracts

Mauthner, M.H.F., Mortensen, J.K., Groat, L.A., and Ercit, T.S. (1995): Geochronology of the Little Nahanni Pegmatite Group and implications for Regional Tectonics. Geological Association of Canada/Mineralogical Association of Canada Program with Abstracts.

Mauthner, M.H.F., Groat, L.A., Ercit, T.S., Mortensen, J.K., and Raudsepp, M. (1994): Mineralogy, Geochemistry, and Geochronology of the Little Nahanni Pegmatite Group, Northwest Territories, Canada. (Abstr.) Geological Society of America/Mineralogical Society of America Program with Abstracts A-222.

Groat, L.A., Ercit, T.S., Raudsepp, M., Mauthner, M.H.F., and Ahlborn, V. (1994): Geology and Mineralogy of the Little Nahanni Pegmatite Group. (Abstr.) Geological Association of Canada/Mineralogical Association of Canada Program with Abstracts A44.

8. BENEFIT TO YUKON

The 1994 field study cost approximately $60,000 ($38,000 from the Canada/Yukon Mineral Development Agreement; if salaries are included, the cost is closer to $100,000). Almost all of this was spent on goods and services in the Yukon Territory, primarily in the communities of Watson Lake, Ross River, and Whitehorse. The bulk of the money went to travel (by truck, floatplane, and helicopter), accommodation, food and supplies.

In November, 1994, the entire Little Nahanni locality (35 km^2) was staked by Canamera Geological Limited of Vancouver. This was done on the basis of our research (but prior to funding by the Canada/Yukon Mineral Development Agreement), but without our knowledge. We have recently learned that a second company was interested in staking the property.

After the staking, one of us (LAG) met with representatives of Canamera Geological Limited to discuss future plans. The company is primarily interested in the Li potential of the property, but also hopes to extract Ta, Nb, Sn, and perhaps Be. Canamera is hoping to improve an old road (to Howard's Pass?) that runs within 15 km of the property. They are planning to do geophysical work and perhaps some drilling in the summer of 1995. All work will be done out of Watson Lake.

9. SUGGESTIONS FOR FUTURE WORK

There are a number of areas that we identified to be of interest that we were unable to visit in 1994. These areas should be looked at in the future to assess their pegmatite potential. The areas are listed below.

9.1 Seagull Batholith (60°10'N, 131°30'W)

The Seagull batholith is a medium-sized (300 km^2) mid-Cretaceous meta- to peraluminous leucocratic granite; with an inital $^{87}Sr/^{86}Sr$ ratio of 0.7120 (Mato *et al.*, 1983). As described by Sinclair and Richardson (1992) it contains quartz-tourmaline orbicules that appear to be the product of a hydrous, B-, F- and Fe-bearing fluid that was trapped in a crystallizing granitic melt.

Anomalous concentrations of Sn (12 to 90 ppm) in the orbicules suggest that this fluid may have been related to the hydrothermal fluids that formed Sn-bearing veins and skarns associated with the Seagull batholith (described by Mato *et al.*, 1983, and others).

The Seagull batholith has relatively high contents of lithophile elements such as Li, Be, Nb, Rb and Ga; F contents range from 0.15 to 0.65%, significantly higher than those of most other granitic rocks (Sinclair and Richardson, 1992).

9.2 Thirtymile Pluton and Ork Stock (60°45'N, 132°15'W)

As described by Liverton (1990), the Thirtymile pluton is roughly elliptical in shape, with a diameter of 8 km. It is made up of four facies: a porphyry, an equigranular microgranite, a megacrystic granite, and a leucocratic topaz- and fluorite-bearing microgranite. The latter contains pale, lithium mica as a major component. Topaz is a common interstitial mineral; fluorite is also common. Tourmaline, apatite, and allanite are occasional accessories. The nearby Ork stock is similar to this facies of the Thirtymile pluton.

9.3 Mount Mye Batholith, Anvil Plutonic Suite (62°20'N, 133°15'W)

As described by Pigage and Anderson (1986), the Mount Mye batholith of the Anvil plutonic suite; near Faro) is a heterogeneous, peraluminous two-mica granite of mid-Cretaceous age (initial $^{87}Sr/^{86}Sr = 0.7405$) that falls within the modal field for granites of the Selwyn suite. However, it is not analogous to the highly-evolved, lithophile-element-enriched siliceous plutons of the Selwyn suite, and therefore may have limited potential as a precursor to rare-element enriched pegmatites.

9.4 Lened, CAC, and RUDI Plutons (NWT; 62°20-25'N, 128°30-40'W)

These plutons are small, massive, composite stocks associated with important tungsten skarns (Dick, 1980). Leucocratic granitic aplite dikes and tourmaline-bearing pegmatite dikes are associated with the plutons. Biotite granite intrusions invade pelitic and calc-silicate hornfels near the CAC and RUDI plutons. They contain muscovite, garnet, andalusite and tourmaline, and some

are miarolitic. These peraluminous dikes seem to be characteristic of plutons with extensive tungsten skarns (Anderson, 1982).

9.5 Sekwi Mountain Map Area (Yukon/NWT; near MacMillan Pass)

A hornblende-absent, biotite bearing pluton has been reported from this area (Anderson, 1983); little is known about it.

9.6 Macmillan Pass (Mactung)

At Mactung, the highest ore grades are associated with zones where quartz veins and aplite and pegmatite dikes are the most abundant, south of the southern margin of the pluton (Atkinson and Baker 1983).

9.7 Mid-Cretaceous Suite, Intermontane Belt (60°40'N, 134°10'W)

Morrison *et al.* (1979) mentions stocks, plugs, and dikes of pegmatitic syenite northeast of Marsh Lake in the Whitehorse map area. The syenite occurs within plutons of the mid-Cretaceous suite in the Intermontane Belt, and as isolated masses in the country rock. However, all initial $^{87}Sr/^{86}Sr$ ratios reported by Morrison *et al.* (1979) for the Whitehorse map area are < 0.7070.

9.8 Emerald Lake (63°36'N, 131°17'W)

In an assessment report by Robertson *et al.* (1981) the Emerald Lake intrusion is described as an elongate, east-west trending body approximately 12 km long and 1.5 to 2.0 km wide. It is primarily syenitic in composition and presumably of Cretaceous age. One part of the intrusion contains a number of very large vugs consisting of large crystals of smoky quartz in a matrix of highly weathered feldspar and mica with minor amounts of arsenopyrite and unidentified minerals believed to be Au-Ag tellurides. Other features indicative of late-stage fluids within the intrusion are the large miarolitic cavities. These range from "incipient vugs" of 10 to 20 cm in diameter to true miarolitic cavities up to 1.5 m in diameter (but 4 m or more in length where they occur as "swells" on a vein) containing quartz crystals up to 1 m in length, tourmaline and mica. In several

areas, well-defined vein systems (seen on cliffs, and described as pegmatites on the map in Roberston *et al.*, 1981) end abruptly and are replaced by a zone of cavities.

9.9 Eastern Margin of the Cassiar Batholith

See section 6.4 for an extended discussion.

10. ACKNOWLEDGEMENTS

Financial support was provided by the Canada/Yukon Mineral Development Agreement (Whitehorse), by the Natural Sciences and Engineering Research Council of Canada in the form of a Research Grant to LAG, by the Canadian Museum of Nature in the form of an RAC Research Grant to TSE, and by the Department of Indian Affairs and Northern Development (Yellowknife).

11. REFERENCES

Aldrich, L.T., Davis, G.L., Titlon, G.R., and Wetherill, G.W. (1956): Radioactive ages of minerals from the Brown Derby Mine and the Quartz Creek Granite near Gunnison, Colorado. *Journal of Geophysical Research,* **61,** 215-232.

Anderson, R.G. (1982): Geology of the Mactung pluton in Niddery Lake map area and some of the plutons in Nahanni map area, Yukon Territory and District of Mackenzie. *In* Current Research, Part A, *Geol. Surv. Can., Pap.* **82-1A,** 299-304.

Anderson, R.G. (1983): Selwyn plutonic suite and its relationship to tungsten skarn mineralization, southeastern Yukon and District of Mackenzie. *In* Current Research, Part B, *Geol. Surv. Can., Pap.* **83-1B,** 151-163.

Anderson, R.G. (1988): An overview of some Mesozoic and Tertiary plutonic suites and their associated mineralization in the northern Cordillera. *In* Recent Advances in the Geology of Granite-Related Mineral Deposits (R.P. Taylor & D.F. Strong, eds.). *Can. Inst. Min. Metall., Spec. Vol.* **39,** 96-113.

Armstrong, R.L. (1988): Mesozoic and early Cenozoic magmatic evolution of the Canadian Cordillera. *In* Processes in Continental Lithosphere Deformation (S.P. Clark, Jr., B.C. Burchfiel and J. Suppe, eds.). *Geol. Soc. Am. Spec. Pap.* **218,** 55-91.

Atkinson, D., and Baker, D.J. (1983): Recent developments in the geologic picture of Mactung: CIM, Mineral Deposits of Northern Cordillera Symposium, 27 (abstr.).

Cerny, P. (1991): Rare-element granitic pegmatites. I. Anatomy and internal evolution of pegmatite deposits. *Geosci. Can.* **18,** 49-67.

Cerny, P., Meintzer, R.E., and Anderson, A.J. (1985): Extreme fractionation in rare-element granitic pegmatites: selected examples of data and mechanisms. *Can. Mineral.* **23,** 381-422.

Dick, L.A. (1980): *A Comparative Study of the Geology, Mineralogy and Conditions of Formation of Contact Metasomatic Mineral Deposits in the Northeastern Canadian Cordillera.* Ph.D. thesis, Queen's Univ., Kingston, Ontario.

Godwin, C.I., Armstrong, R.L., and Tompson, K.M. (1980): K-Ar and Rb-Sr dating and the genesis of tungsten at the Clea tungsten skarn property, Selwyn Mountains, Yukon territory. *Can. Inst. Min. Metall., Bull.* **73,** 90-93.

Godwin, C.I., and Sinclair, A.J. (1982): Average lead isotope growth curves for shale-hosted zinc-lead deposits, Canadian Cordillera. *Economic Geology,* **7,** 675-690.

Gordey, S.P., and Anderson, R.G. (1993): Evolution of the northern Cordilleran miogeocline, Nahanni map area (105I), Yukon and Northwest Territories. *Geol. Surv. Can., Mem.* **428**

Keppler, H. (1993): Influence of fluorine on the enrichment of high field strength trace elements in granitic rocks. *Contrib. Mineral. Petrol.* **114**, 479-488.

Liverton, T. (1990): Tin-bearing skarns of the Thirtymile Range: a progress report. *In* Yukon Geology, vol. 3, Exploration and Geological Services Division, Yukon Territory, Department of Indian and Northern Affairs, 52-70.

London, D. (1984): Experimental phase equilibria in the system $LiAlSiO_4$-SiO_2-H_2O: a petrogenetic grid for lithium-rich pegmatites. *Am. Mineral.* **69,** 995-1004.

Mato, G., Ditson, G., and Godwin, C. (1983): Geology and geochronometry of tin mineralization associated with the Seagull batholith, south-central Yukon Territory. *Can. Inst. Min. Metall., Bull.* **76,** 43-49.

Morrison, G.W., Godwin, C.I., and Armstrong, R.L. (1979): Interpretation of isotopic ages and initial $^{87}Sr/^{86}Sr$ ratios for plutonic rocks in the Whitehorse map area, Yukon. *Can. J. Earth Sci.* **16,** 1988-1997.

Mulligan, R. (1968): Geology of Canadian beryllium deposits. *Geol. Surv. Can., Econ. Geol. Rept.* **23,**

Murphy, D.C., and Héon, D. (1994): Geological overview of Sprague Creek map area, western Selwyn Basin. *In* Yukon Exploration and Geology 1993, Exploration and Geological Services Division, Department of Indian Affairs and Northern Development, 29-46.

Murphy, D.C., Mortensen, J.K., and Bevier, M.L. (1995): U-Pb and K-Ar geochronology of Cretaceous and Tertiary intrusions, western Selwyn Basin, and implications for the structural and metallogenic evolution of central Yukon. *In* Geological Association of Canada, Program with Abstracts, **20**.

Pigage, L.C., and Anderson, R.G. (1986): The Anvil plutonic suite, Faro, Yukon Territory. *Can. J. Earth Sci.* **22,** 1204-1216.

Robertson, R.C.R., Doherty, R.A., and Garagan, T. (1981): Assessment report for Ice Claims; AGIP Canada Ltd.

Romer, R.L., and Wright, J.E. (1992): U-Pb dating of columbites: A geochronologic tool to date magmatism and ore deposits. *Geochimica et Cosmochimica Acta,* **56,** 2137-2142.

Sinclair, W.D., and Richardson, J.M. (1992): Quartz-tourmaline orbicules in the Seagull batholith, Yukon Territory. *Can. Mineral.* **30,** 923-936.

Tompson, K.M. (1978): *Geology of the Clea Tungsten Deposit, Yukon Territory.* B.Sc. thesis, Univ. of British Columbia, Vancouver, British Columbia.

White, A.J.R., and Chappell, B.W. (1983): Granitoid types and their distibution in the Lachlan Fold Belt, southeastern Australia. *In* Circum-Pacific Plutonic Terranes (J.A. Roddick, ed.). *Geol. Soc. Am., Mem.* **159,** 21-34.

APPENDIX 1: MINERAL ANALYSES

Feldspar Samples

1. K-feldspar, Li-pegmatite dyke in O'Grady batholith
2. K-feldspar, Li-pegmatite dyke in O'Grady batholith (cryptoperthite matrix)
3. K-feldspar, pegmatite dyke in O'Grady batholith (microperthite matrix)
4. Albite, Li-pegmatite dyke in O'Grady batholith (associated with Kfp #1)
5. Albite, pegmatite dyke in O'Grady batholith (lamella in Kfp #3)
6, 7. Albite, pegmatite dyke in O'Grady batholith (2 spots in one sample)

Lepidolite Samples

8. Li-pegmatite dyke in O'Grady batholith

Titanite Samples

9. Pegmatite dyke, O'Grady batholith (grain #1)
10. Pegmatite dyke, O'Grady batholith (grain #2)

Zircon Samples

11-14. Four analyses of one grain, pegmatite dyke in O'Grady batholith
(11-13: core, 14: rim)

Axinite Samples

15. Ferroaxinite, pegmatite dyke in O'Grady batholith

Tourmaline Samples

16. Elbaite, Li-pegmatite dyke in O'Grady batholith
(sample #1, gem red)
17. Elbaite, Li-pegmatite dyke in O'Grady batholith
(sample #1, gem pink)
18. Lithian schorl, Li-pegmatite dyke in O'Grady batholith
(sample #2, blue-black core)
19. Elbaite, Li-pegmatite dyke in O'Grady batholith
(sample #2, gem red rim)
20. Ferroan elbaite, Li-pegmatite dyke in O'Grady batholith
(sample #3, green-black core)
21. Elbaite, Li-pegmatite dyke in O'Grady batholith
(sample #4, late-generation, pink gem core)
22. Elbaite, Li-pegmatite dyke in O'Grady batholith
(sample #4, pink gem rim)
23. Schorl, pegmatite dyke in O'Grady batholith
(sample #5, black)
24. Schorl, pegmatite dyke in O'Grady batholith
(sample #6, black)
25. Schorl, pegmatite dyke in O'Grady batholith
(sample #6, black)
26. Schorl, pegmatite dyke in O'Grady batholith
(sample #6, black)
27. Schorl, hydrothermal quartz-tourmaline vein, Clea pluton
(sample #7, Mg-Fe zoned, black)
28. Schorl, hydrothermal quartz-tourmaline vein, Clea pluton
(sample #7, Mg-Fe zoned, black)

Cassiterite Samples

29. Hydrothermal quartz vein, Clea pluton

Wolframite Samples

30-31. Ferberite, Clea pluton
(two analyses, one sample)

Scheelite Samples

32. At contact of aplite dyke, Clea pluton (sample #1)
33. Hydrothermal quartz vein, Clea pluton (sample #2)

Apatite (Fluorapatite) Samples

34. Greisen, Clea Pluton (sample #1, zoned, core)
35. Greisen, Clea Pluton (sample #1, zoned, outer zone)
36. Hydrothermal quartz vein, Clea pluton (sample #2)

Hambergite Samples

37. Li-pegmatite dyke in O'Grady batholith
(inclusion in elbaite)

TABLE 1. CHEMICAL COMPOSITION OF SILICATE MINERALS (LESS TOURMALINE)

	1	2	3	4	5	6	7	8	9	10	11	12	13	14	15
SiO2	65.11	63.67	64.81	69.04	68.68	65.16	67.66	60.77	30.12	30.76	30.93	30.90	31.16	31.09	42.21
TiO2	---	---	---	---	---	---	---	---	34.18	31.78	0.00	0.00	0.00	0.00	0.00
SnO2	---	---	---	---	---	---	---	---	0.00	0.15	---	---	---	---	---
ZrO2	---	---	---	---	---	---	---	---	---	---	55.61	57.79	59.89	62.02	---
HfO2	---	---	---	---	---	---	---	---	---	---	1.56	1.74	1.78	2.02	---
ThO2	---	---	---	---	---	---	---	---	---	---	1.43	1.02	0.47	1.47	---
UO2	---	---	---	---	---	---	---	---	---	---	8.73	7.96	5.65	1.50	---
Nb2O5	---	---	---	---	---	---	---	---	0.28	1.68	---	---	---	---	---
Ta2O5	---	---	---	---	---	---	---	---	0.49	0.69	---	---	---	---	---
B2O3*	---	---	---	---	---	---	---	---	---	---	---	---	---	---	6.11
Al2O3	18.39	18.61	18.39	19.70	19.75	21.19	19.90	15.90	2.35	3.70	0.00	0.00	0.00	0.62	17.62
V2O3	---	---	---	---	---	---	---	---	---	---	---	---	---	---	0.00
Fe2O3	0.00	0.00	0.10	0.00	0.06	0.00	0.00	---	---	---	---	---	---	---	---
Y2O3	---	---	---	---	---	---	---	---	---	---	0.94	0.86	0.67	0.26	---
Yb2O3	---	---	---	---	---	---	---	---	---	---	0.00	0.40	0.00	0.00	---
MgO	---	---	---	---	---	---	---	0.00	0.00	0.00	---	---	---	---	1.29
MnO	0.00	0.00	0.00	0.00	0.00	0.00	0.00	0.08	0.08	0.19	0.00	0.00	0.00	0.00	1.66
FeO	---	---	---	---	---	---	---	0.08	2.23	2.39	0.00	0.00	0.00	0.29	9.30
CaO	0.00	0.00	0.00	0.00	0.10	0.87	0.38	0.00	27.58	27.97	0.00	0.00	0.00	0.08	19.50
SrO	0.09	0.10	0.10	0.00	0.05	0.05	0.00	0.00	---	---	---	---	---	---	---
BaO	0.00	0.00	0.00	0.00	0.00	0.00	0.00	0.00	---	---	---	---	---	---	---
Li2O*	---	---	---	---	---	---	---	7.46	---	---	---	---	---	---	---
Na2O	0.30	0.25	0.64	11.84	11.50	10.92	11.52	0.00	---	---	0.00	0.00	0.00	0.00	0.00
K2O	16.92	16.82	16.13	0.05	0.16	0.07	0.00	11.64	---	---	0.00	0.00	0.00	0.00	0.00
Rb2O	0.21	0.25	0.06	0.00	0.00	0.00	0.00	0.00	---	---	---	---	---	---	---
Cs2O	0.06	0.06	0.00	0.00	0.00	0.00	0.00	0.39	---	---	---	---	---	---	---
F	---	---	---	---	---	---	---	8.93	0.78	1.25	---	---	---	---	0.00
H2O*	---	---	---	---	---	---	---	0.46	0.77	0.56	---	---	---	---	1.58
O=F	---	---	---	---	---	---	---	-3.76	-0.33	-0.53	---	---	---	---	---
	101.08	99.76	100.23	100.63	100.30	98.26	99.46	101.95	98.53	100.59	99.20	100.67	99.62	99.35	99.27

FORMULA CONTENTS

Si	2.994	2.972	2.993	2.995	2.990	2.906	2.973	3.880	3.970	3.988	1.012	0.997	0.997	0.981	4.004
Ti	---	---	---	---	---	---	---	---	3.388	3.098	0.000	0.000	0.000	0.000	0.000
Sn	---	---	---	---	---	---	---	---	0.000	0.009	---	---	---	---	---
Zr	---	---	---	---	---	---	---	---	---	---	0.887	0.909	0.934	0.954	---
Hf	---	---	---	---	---	---	---	---	---	---	0.015	0.016	0.016	0.018	---
Th	---	---	---	---	---	---	---	---	---	---	0.011	0.007	0.003	0.011	---
U	---	---	---	---	---	---	---	---	---	---	0.064	0.057	0.040	0.011	---
Nb	---	---	---	---	---	---	---	---	0.017	0.098	---	---	---	---	---
Ta	---	---	---	---	---	---	---	---	0.018	0.024	---	---	---	---	---
B*	---	---	---	---	---	---	---	---			---	---	---	---	1.000
Al	0.997	1.024	1.001	1.007	1.014	1.114	1.030	1.196	0.365	0.565	0.000	0.000	0.000	0.023	1.970
V	---	---	---	---	---	---	---	---	---	---	---	---	---	---	0.000
Fe3+	0.000	0.000	0.003	0.000	0.002	0.000	0.000	---	---	---	---	---	---	---	---
Y	---	---	---	---	---	---	---	---	---	---	0.016	0.015	0.011	0.004	---
Yb	---	---	---	---	---	---	---	---	---	---	0.000	0.004	0.000	0.000	---
Mg	---	---	---	---	---	---	---	---	0.000	0.000	---	---	---	---	0.182
Mn	0.000	0.000	0.000	0.000	0.000	0.000	0.000	0.004	0.009	0.021	0.000	0.000	0.000	0.000	0.133
Fe2+	---	---	---	---	---	---	---	0.004	0.246	0.259	0.000	0.000	0.000	0.008	0.738
Ca	0.000	0.000	0.000	0.000	0.005	0.042	0.018		3.895	3.885	0.000	0.000	0.000	0.003	1.982
Sr	0.002	0.003	0.003	0.000	0.001	0.001	0.000	0.000	---	---	---	---	---	---	---
Ba	0.000	0.000	0.000	0.000	0.000	0.000	0.000	0.000	---	---	---	---	---	---	---
Li*	---	---	---	---	---	---	---	1.915	---	---	---	---	---	---	---
Na	0.027	0.023	0.057	0.996	0.971	0.944	0.981	---	---	---	0.000	0.000	0.000	0.000	0.000
K	0.993	1.002	0.950	0.003	0.009	0.004	0.000	0.948	---	---	0.000	0.000	0.000	0.000	0.000
Rb	0.006	0.008	0.002	0.000	0.009	0.000	0.000	0.000	---	---	---	---	---	---	---
Cs	0.001	0.001	0.000	0.000	0.000	0.000	0.000	0.011	---	---	---	---	---	---	---
	5.020	5.033	5.009	5.001	4.992	5.011	5.002	7.958	11.908	11.947	2.005	2.005	2.001	2.013	10.009
F	---	---	---	---	---	---	---	1.803	0.325	0.512	---	---	---	---	0.000
OH*	---	---	---	---	---	---	---	0.197	0.675	0.488	---	---	---	---	1.000
O	8.000	8.000	8.000	8.000	8.000	8.000	8.000	10.000	19.000	19.000	4.000	4.000	4.000	4.000	15.000
	8.000	8.000	8.000	8.000	8.000	8.000	8.000	12.000	20.000	20.000	4.000	4.000	4.000	4.000	16.000

1-3: K-feldspar (formulae on a basis of 8 O), 4-7: plagioclase (8 O), 8: lepidolite, 9-10: titanite (20 anions), 11-14: zircon (4 O), 15: ferroaxinite (16 anions). "0.00": not detected, "---": not measured, "*": calculated for stoichiometry.

TABLE 2. CHEMICAL COMPOSITION OF TOURMALINE SAMPLES

	16	17	18	19	20	21	22	23	24	25	26	27	28
SiO2	36.81	36.85	34.83	37.24	35.83	36.98	35.86	33.56	33.55	33.72	33.63	33.55	35.51
TiO2	0.00	0.00	0.61	0.00	0.60	0.00	0.00	1.80	1.43	1.44	0.87	0.69	0.28
B2O3*	11.00	11.04	10.29	10.97	10.51	10.92	10.66	9.65	9.69	9.74	9.78	10.14	10.39
Al2O3	41.28	42.04	33.71	39.34	35.05	40.00	38.00	22.43	24.45	24.64	25.69	32.76	33.61
V2O3	0.00	0.00	0.00	0.00	0.00	0.00	0.00	0.09	0.00	0.08	0.00	0.00	0.00
MgO	0.00	0.00	0.00	0.00	0.07	0.00	0.00	3.32	1.78	1.61	3.57	1.56	2.08
MnO	0.21	0.11	0.86	3.28	0.81	1.85	4.19	0.36	0.33	0.33	0.27	0.15	0.15
FeO	0.00	0.10	11.06	0.40	8.53	0.42	0.81	20.84	21.23	21.39	17.64	14.27	12.56
CaO	1.96	1.16	0.34	1.08	0.34	0.98	0.74	1.75	1.23	1.25	1.46	0.68	0.22
Li2O*	2.30	2.17	0.95	1.97	1.29	2.03	1.76	0.00	0.00	0.00	0.00	0.00	0.00
Na2O	1.56	1.93	2.71	2.39	2.83	2.23	2.83	1.86	2.13	2.11	2.01	1.81	1.65
K2O	0.00	0.00	0.00	0.00	0.00	0.00	0.00	0.07	0.04	0.06	0.05	0.04	0.00
F	1.58	1.13	1.43	1.57	1.30	1.27	2.33	0.51	0.48	0.00	0.62	0.00	0.00
H2O*	3.04	3.27	2.87	3.04	3.01	3.16	2.57	3.09	3.12	3.36	3.08	3.50	3.58
O=F	-0.67	-0.48	-0.60	-0.66	-0.55	-0.53	-0.98	-0.21	-0.20	0.00	-0.26	0.00	0.00
	99.07	99.32	99.06	100.62	99.62	99.31	98.77	99.12	99.26	99.73	98.41	99.15	100.03
						FORMULA CONTENTS PER 31 ANIONS							
Si	5.818	5.799	5.883	5.902	5.925	5.888	5.849	6.046	6.019	6.019	5.978	5.750	5.942
Ti	0.000	0.000	0.077	0.000	0.075	0.000	0.000	0.244	0.193	0.193	0.116	0.089	0.035
B*	3.000	3.000	3.000	3.000	3.000	3.000	3.000	3.000	3.000	3.000	3.000	3.000	3.000
Al	7.689	7.798	6.711	7.349	6.831	7.506	7.305	4.762	5.169	5.184	5.382	6.617	6.628
V	0.000	0.000	0.000	0.000	0.000	0.000	0.000	0.013	0.000	0.011	0.000	0.000	0.000
Mg	0.000	0.000	0.000	0.000	0.017	0.000	0.000	0.892	0.476	0.428	0.946	0.399	0.519
Mn	0.028	0.015	0.123	0.440	0.113	0.249	0.579	0.055	0.050	0.050	0.041	0.022	0.021
Fe	0.000	0.013	1.562	0.053	1.180	0.056	0.110	3.140	3.185	3.193	2.622	2.045	1.758
Ca	0.332	0.196	0.062	0.183	0.060	0.167	0.129	0.338	0.236	0.239	0.278	0.125	0.039
Li*	1.462	1.373	0.645	1.256	0.858	1.300	1.155	0.000	0.000	0.000	0.000	0.000	0.000
Na	0.478	0.589	0.887	0.734	0.907	0.688	0.895	0.650	0.741	0.730	0.693	0.601	0.535
K	0.000	0.000	0.000	0.000	0.000	0.000	0.000	0.016	0.009	0.014	0.011	0.009	0.000
	18.807	18.783	18.950	18.917	18.966	18.854	19.022	19.156	19.078	19.061	19.067	18.657	18.477
F	0.790	0.562	0.764	0.787	0.680	0.639	1.202	0.291	0.272	0.000	0.349	0.000	0.000
OH*	3.210	3.438	3.236	3.213	3.320	3.361	2.798	3.709	3.728	4.000	3.651	4.000	4.000
O	27.000	27.000	27.000	27.000	27.000	27.000	27.000	27.000	27.000	27.000	27.000	27.000	27.000
	31.000	31.000	31.000	31.000	31.000	31.000	31.000	31.000	31.000	31.000	31.000	31.000	31.000

0.00: not detected, "*": calculated for stoichiometry.

TABLE 3. CHEMICAL COMPOSITION OF NON-SILICATE MINERALS

	29	30	31	32	33	34	35	36	37
WO3	0.00	75.83	75.75	81.74	81.77	---	---	---	---
P2O5	---	---	---	---	---	42.82	42.95	43.35	---
Nb2O5	0.00	0.00	0.00	0.00	0.00	---	---	---	---
Ta2O5	0.71	0.00	0.00	0.00	0.00	---	---	---	---
SiO2		---	---	---	---	0.10	0.11	0.00	---
TiO2	0.79	0.00	0.00	0.00	0.00	---	---	---	---
SnO2	99.23	0.00	0.00	0.00	0.00	---	---	---	---
B2O3*	---	---	---	---	---	---	---	---	36.95
Ce2O3	---	---	---	---	---	0.00	0.19	0.21	---
BeO*	---	---	---	---	---	---	---	---	53.10
MgO	0.00	0.09	0.08	0.00	0.00	0.00	0.00	0.00	---
MnO	0.00	6.31	6.49	0.00	0.00	0.23	0.22	0.26	---
FeO	0.00	17.36	17.32	0.00	0.00	0.10	0.09	0.11	---
CaO	0.00	0.00	0.00	18.96	19.67	55.20	55.40	55.86	---
SrO	---	---	---	---	---	0.09	0.08	0.00	---
F	---	---	---	---	---	3.00	3.60	3.70	3.61
Cl	---	---	---	---	---	0.00	0.00	0.00	---
H2O*	---	---	---	---	---	0.38	0.10	0.07	7.85
O=F	---	---	---	---	---	-1.26	-1.52	-1.56	-1.52
	100.73	99.59	99.64	100.70	101.44	100.66	101.22	101.99	99.99

FORMULA CONTENTS

W	---	0.996	0.994	1.010	1.001	---	---	---	---
P	---	---	---	---	---	3.015	3.012	3.018	---
Nb	0.000	0.000	0.000	0.000	0.000	---	---	---	---
Ta	0.005	0.000	0.000	0.000	0.000	---	---	---	---
Si	---	---	---	---	---	0.008	0.009	0.000	---
Ti	0.015	0.000	0.000	0.000	0.000	---	---	---	---
Sn	0.979	0.000	0.000	0.000	0.000	---	---	---	---
B*	---	---	---	---	---	---	---	---	1.000
Ce	---	---	---	---	---	0.000	0.006	0.006	
Be*	---	---	---	---	---	---	---	---	2.000
Mg	---	0.007	0.006	0.000	0.000	---	---	---	---
Mn	---	0.271	0.278	0.000	0.000	0.016	0.015	0.018	---
Fe	---	0.736	0.733	0.000	0.000	0.007	0.006	0.008	---
Ca	---	0.000	0.000	0.969	0.996	4.919	4.917	4.921	---
Sr	---	---	---	---	---	0.004	0.004	0.000	---
	0.999	2.010	2.011	1.979	1.997	7.969	7.969	7.971	3.000
F	---	---	---	---	---	0.789	0.943	0.962	0.179
Cl	---	---	---	---	---	0.000	0.000	0.000	---
OH*	---	---	---	---	---	0.211	0.057	0.038	0.821
O	2.000	4.000	4.000	4.000	4.000	12.000	12.000	12.000	3.000
	2.000	4.000	4.000	4.000	4.000	13.000	13.000	13.000	4.000

29: cassiterite (formula on basis of 2 O), 30-31: wolframite (4 O),
32-33: scheelite (4 O), 34-36: apatite (13 anions), 37: hambergite (4 anions)
"0.00": not detected, "---": not measured, "*": calculated for stoichiometry

LIST OF FIGURES

Fig. 1

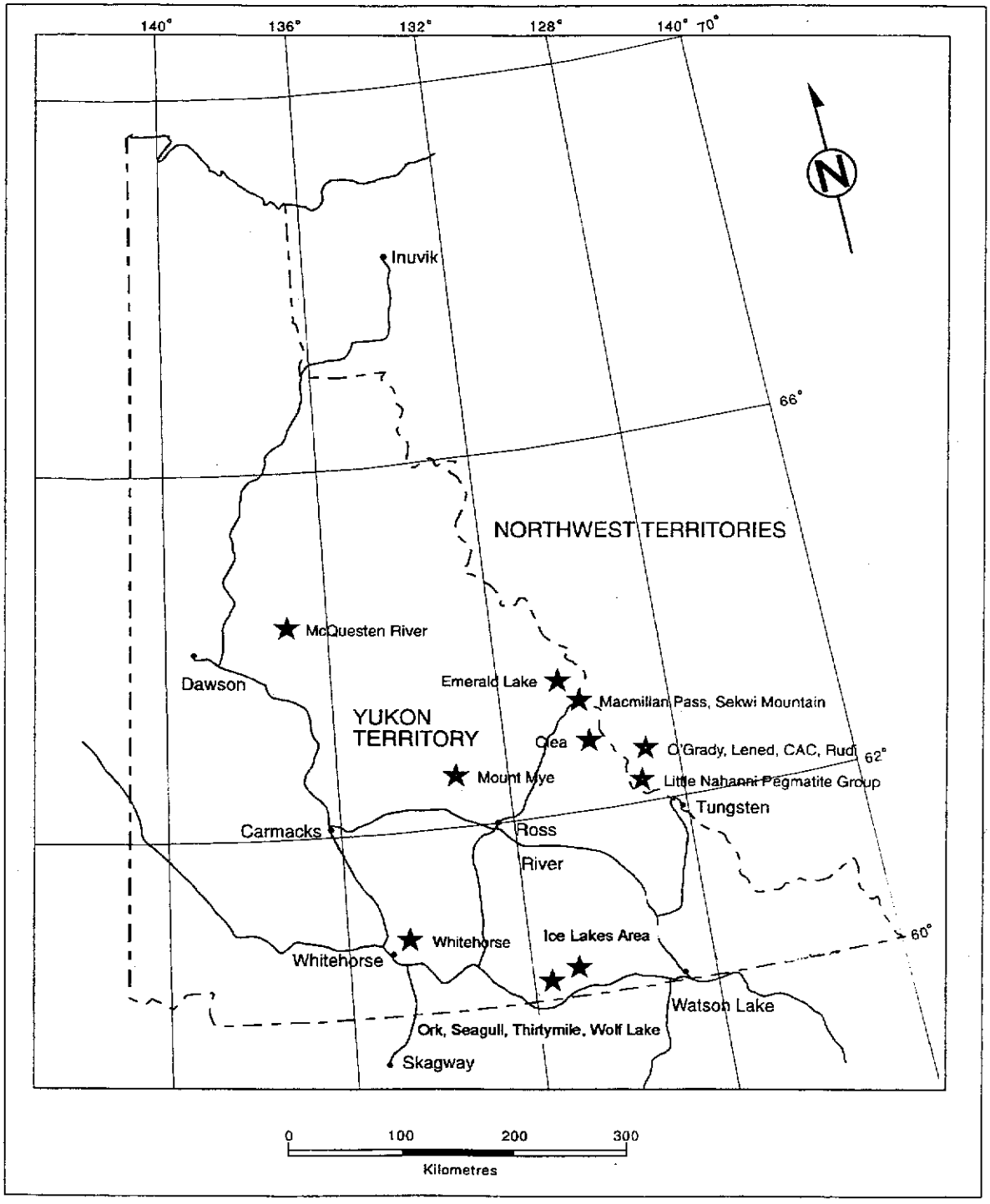
140°
136°
132°
128°
140°
70°
N
Inuvik
66°
NORTHWEST TERRITORIES
McQuesten River
Dawson
Emerald Lake
Macmillan Pass, Sekwi Mountain
YUKON
TERRITORY
Clea
O'Grady, Lened, CAC, Rud
62°
Mount Mye
Little Nahanni Pegmatite Group
Tungsten
Carmacks
Ross
River
Whitehorse
Ice Lakes Area
Whitehorse
60°
Watson Lake
Ork, Seagull, Thirtymile, Wolf Lake
Skagway
0
100
200
300
Kilometres

Fig. 2

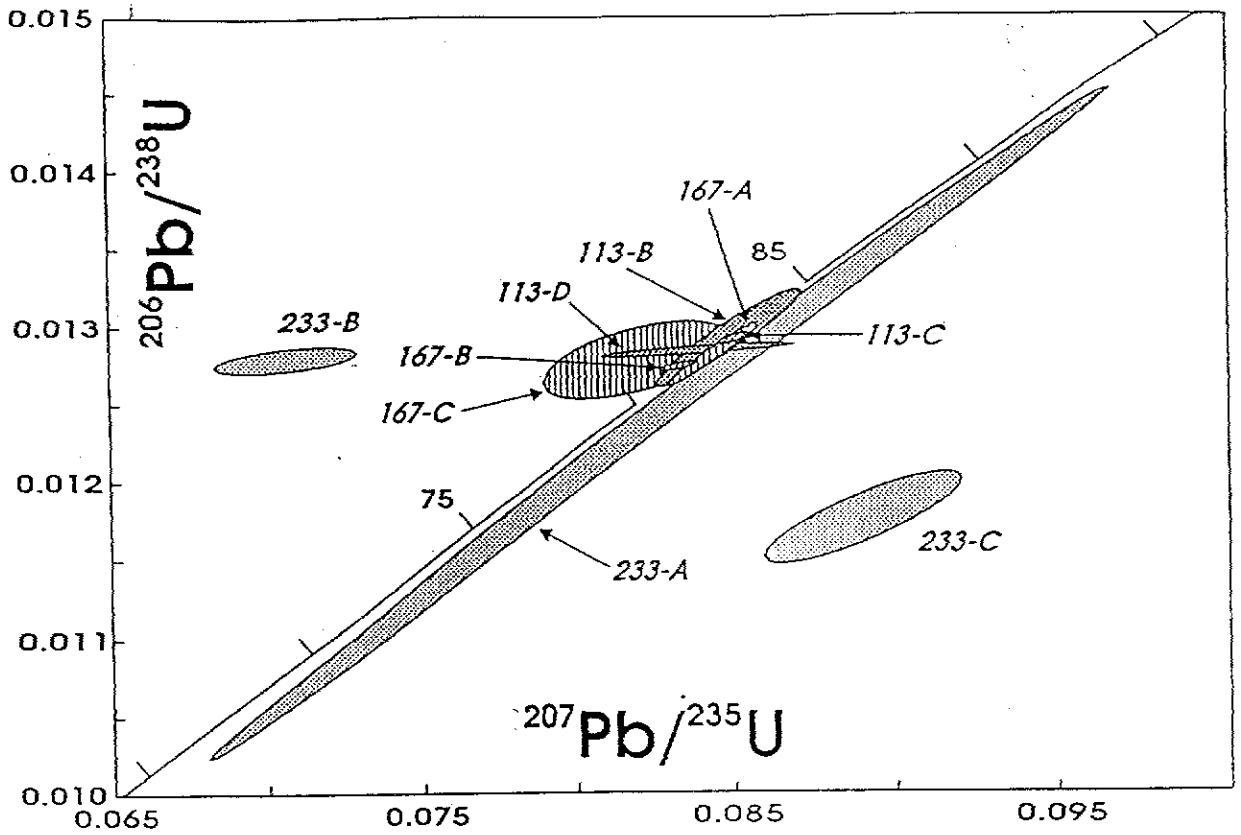
0.015
0.014
0.013
0.012
0.011
0.010
0.065
0.075
0.085
0.095
$^{206}Pb/^{238}U$
$^{207}Pb/^{235}U$
167-A
113-B
85
113-D
233-B
167-B
113-C
167-C
75
233-A
233-C

Fig. 3

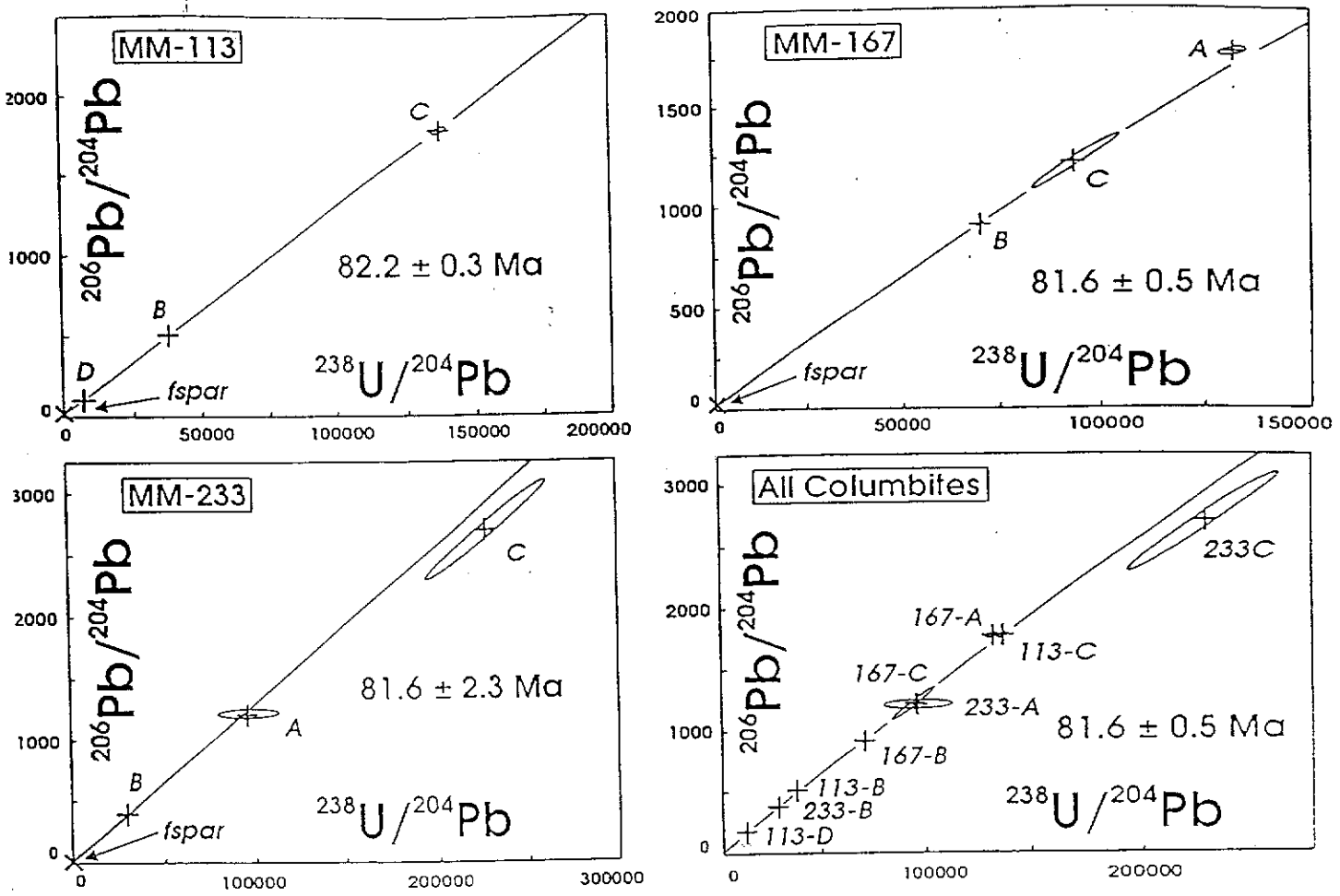
MM-113
82.2 ± 0.3 Ma
MM-167
81.6 ± 0.5 Ma
MM-233
81.6 ± 2.3 Ma
All Columbites
81.6 ± 0.5 Ma
fspar
$^{206}Pb/^{204}Pb$
$^{238}U/^{204}Pb$

Fig. 4

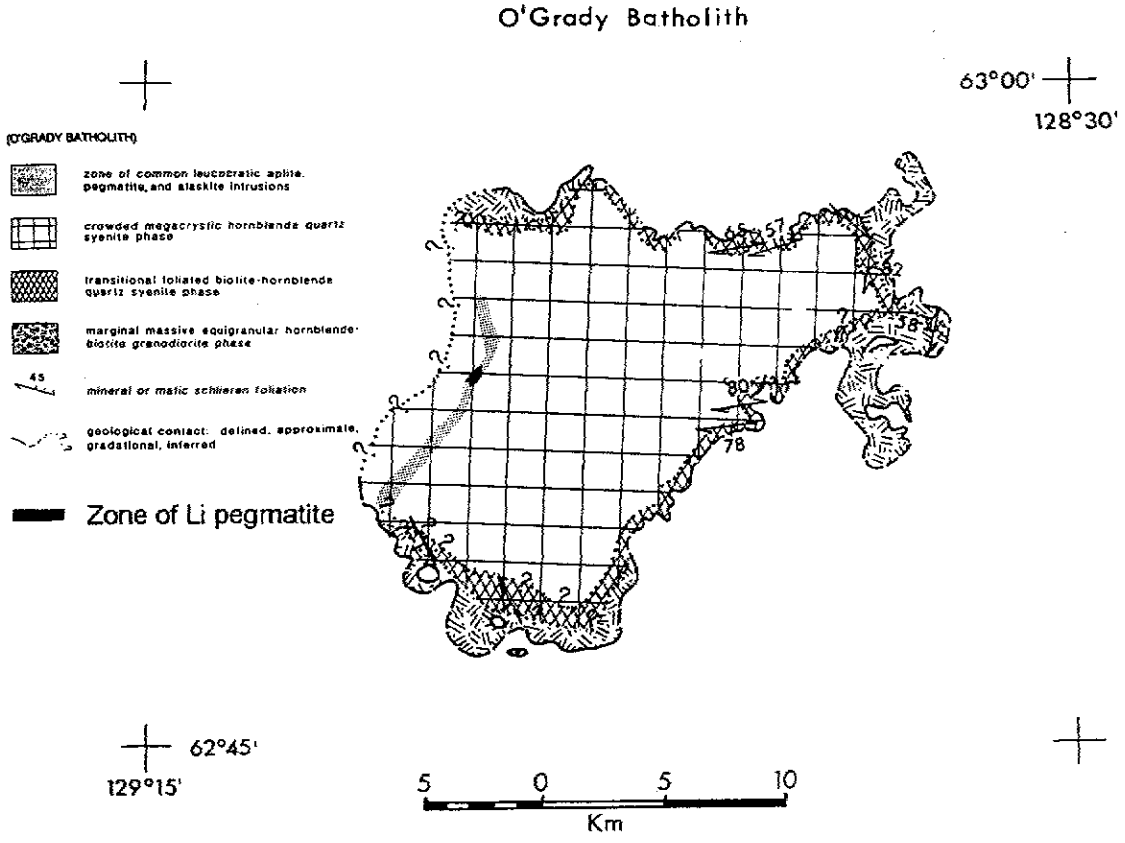
O'Grady Batholith
63°00'
128°30'
(O'GRADY BATHOLITH)
zone of common leucocratic aplite, pegmatite, and alaskite intrusions
crowded megacrystic hornblende quartz syenite phase
transitional foliated biotite-hornblende quartz syenite phase
marginal massive equigranular hornblende-biotite granodiorite phase
45
mineral or mafic schlieren foliation
geological contact: defined, approximate, gradational, inferred
Zone of Li pegmatite
62°45'
129°15'
5 0 5 10
Km

Fig. 5

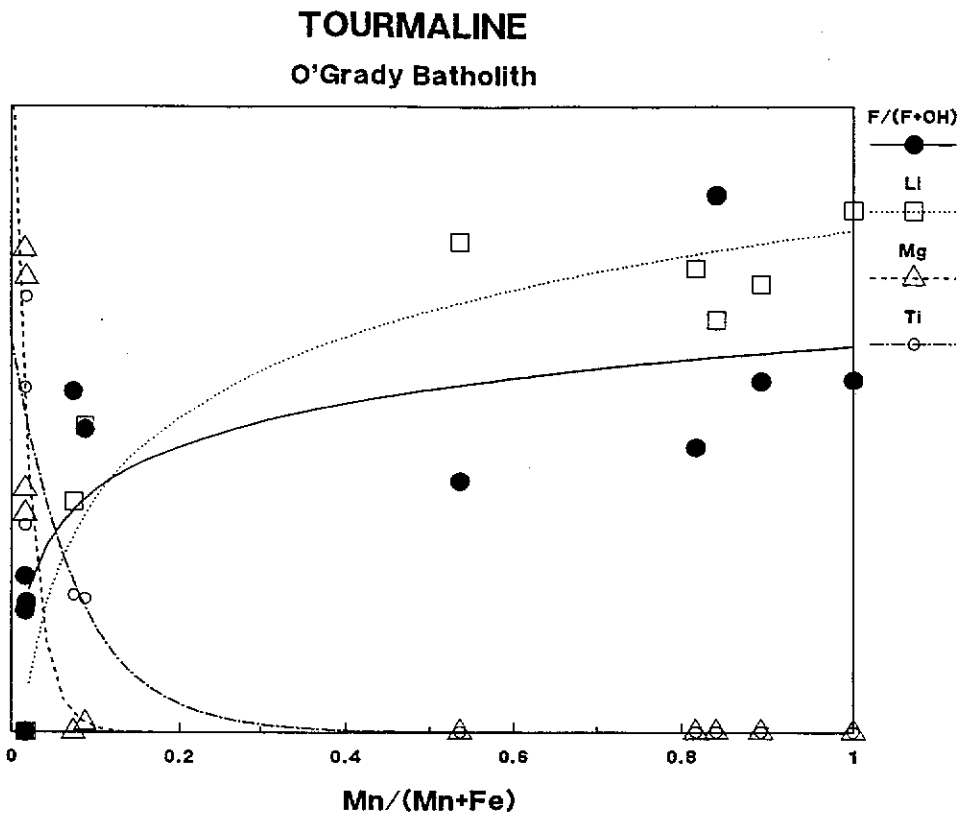
TOURMALINE
O'Grady Batholith
F/(F+OH)
Li
Mg
Ti
0
0.2
0.4
0.6
0.8
1
Mn/(Mn+Fe)

Fig. 6

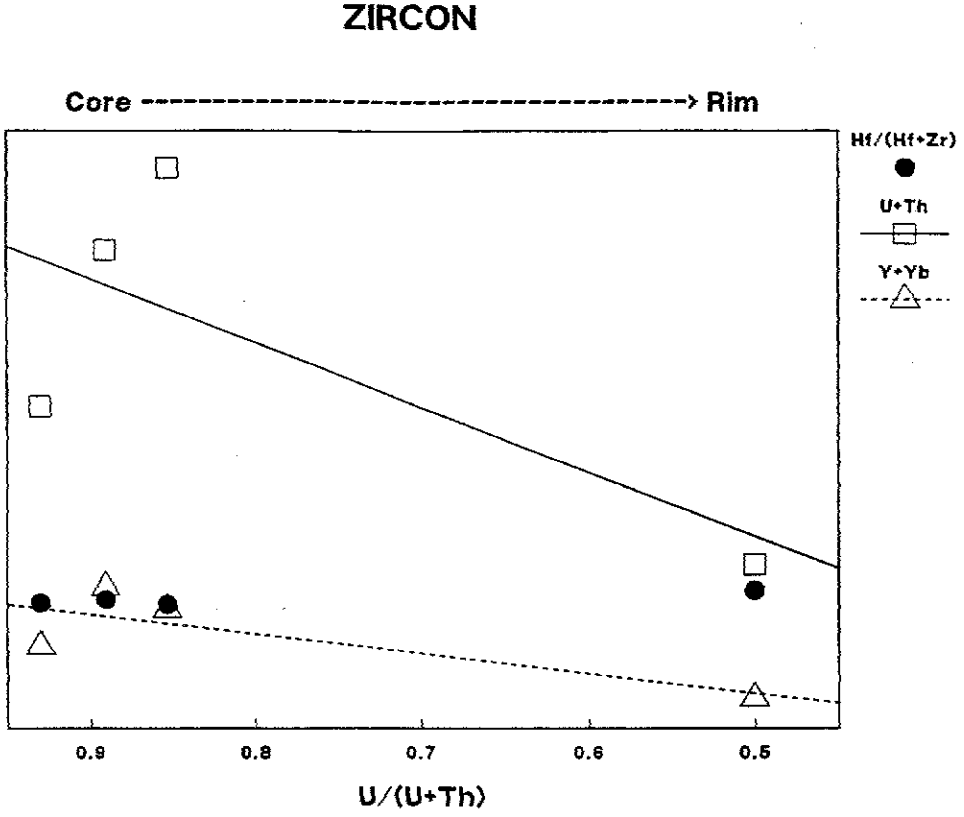

Fig. 7

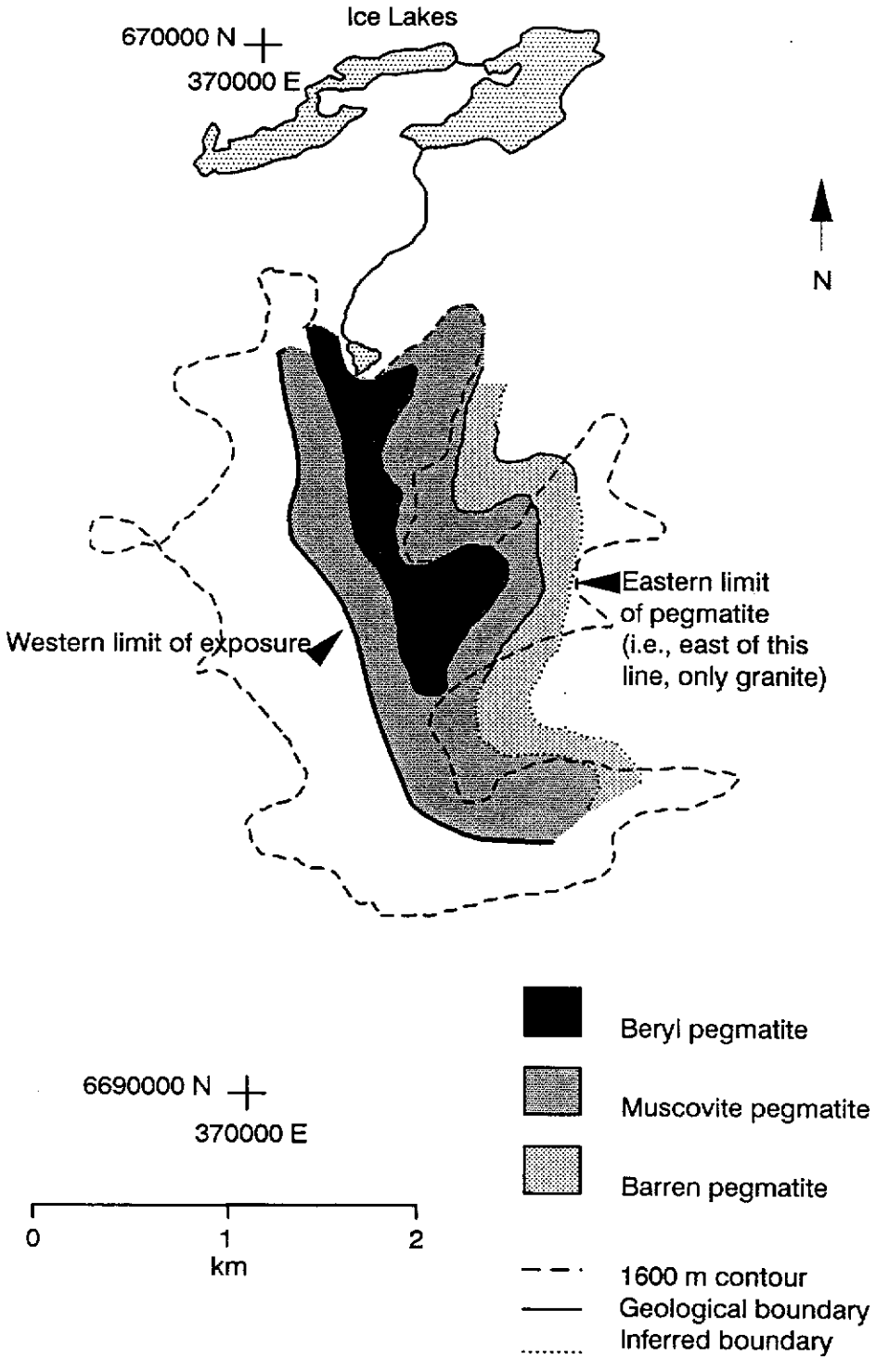
Ice Lakes
670000 N
370000 E
N
Eastern limit
of pegmatite
(i.e., east of this
line, only granite)
Western limit of exposure
Beryl pegmatite
Muscovite pegmatite
Barren pegmatite
6690000 N
370000 E
0
1
2
km
1600 m contour
Geological boundary
Inferred boundary